Green OA (self-archived) version of
HOHMANN, N, 2021, INCORPORATING INFORMATION ON VARYING SEDIMENTATION RATES INTO PALEONTOLOGICAL ANALYSES: PALAIOS 36 (2): 53–67, DOI: http://dx.doi.org/10.2110/palo.2020.038, https://pubs.geoscienceworld.org/sepm/palaios/article-abstract/36/2/53/594922/INCORPORATING-INFORMATION-ON-VARYING-SEDIMENTATION
When citing this text please use the above reference!
Contact:
NIKLAS HOHMANN
Friedrich-Alexander-Universität Erlangen-Nürnberg, GeoZentrum Nordbayern, Institut für Paläoumwelt, 91054 Erlangen, Germany
email: Niklas.Hohmann@fau.de

Plain Language Summary

Fossil accumulations can be generated by (1) ecologically important events such as blooms in productivity, or by (2) low sedimentation rates that reduce the spacing between individual fossils. The latter case, known as sedimentary condensation, affects not only fossils, but all information recorded by the sedimentary rock record. A first step towards the correct attribution of changes is fossil abundance is a quantitative description of the sedimentary expression resulting from varying sedimentation and shell input rates.
I present the DAIME model, a method to incorporate the effects of changing sedimentation rates into paleontological analyses. It is implemented for R Software and available as a package on CRAN. It is complemented by a statistical framework to assess how uncertainties about sedimentary conditions affect the results of the model.
As an application, I examine a clustering of species disappearances on Seymour Island, Antarctica, approximately 250 thousand years before the Cretaceous/Paleogene boundary. Modeling a range extinction and sedimentation scenarios shows that the clustering can be equally attributed to
(1) an extinction event that is potentially linked to Deccan volcanism and
(2) an extended period of low sedimentation rates, leading to a condensation of background extinctions.
The model allows quantifying whether these two possible causes can be distinguished, given the available data. This example application illustrates a quantitative evaluation of a long-standing argument on whether the Cretaceous/Paleogene boundary was associated with a single-peaked or a double-peaked extinction event.

Kurzzusammenfassung

Ansammlungen von Fossilien können sowohl durch ökologisch bedeutsame Ereignisse wir erhöhte Produktivität als auch durch reduzierte Sedimentationsraten erzeugt werden, welche den Abstand zwischen den einzelnen Fossilien reduziert. Dieser als sedimentäre Kondensation bezeichnete Effekt betrifft alle Informationen welche durch Sedimente vermittelt werden können. Ein erster Schritt zur korrekten Einordnung von Fossilansammlungen ist eine quantitative Beschreibung der stratigraphischen Muster welche durch eine Kombination von veränderlichem Eintrag von Sediment und Überresten vergangenen Lebens erzeugt werden.
In dieser Publikation präsentiere Ich das DAIME Modell, welches ermöglicht die Effekte von veränderlichen Sedimentationsraten mit in paläontologische Analysen einzubeziehen. Das Modell ist für die R Software implementiert und steht auf CRAN zum Download zur Verfügung. Zusätzliche stelle Ich eine Methode vor welche erlaubt die Variantionen in den

Ergebnissen des Modells bei Unsicherheiten der Sedimentationsbedingungen zu analysieren.

Als Anwendung untersuche ich das gehäufte Verschwindend von Arten auf Seymour Island (Antarktis) ungefähr 250 tausend Jahre vor der Kreide-Paläogen-Grenze. Durch Modellierung einer Reihe von Sedimentations- und Aussterbeszenarios zeige ich, dass diese Anhäufung sowohl durch

(1) ein Aussterbeereignis, welches potentiell durch den zeitgleichen Deccan-Vulkanismus verursacht wurde,

als auch durch

(2) eine verlängerte Periode von niedrigen Sedimentationsraten, welche zur sedimentären Kondensation der Hintergrundaussterberate führt,

erklärt werden kann.

Das entwickelte Modell erlaubt zu unterscheiden ob diese beiden Szenarien auf der Basis der vorhandenen Daten unterschieden werden kann. Dieses Beispielanwendung demonstriert wie die seit langem andauernden Diskussion ob die Kreide-Paläogen-Grenze mit einem oder zwei Aussterbeereignissen einher ging quantitativ analysiert werden kann.

ABSTRACT

Stratigraphic changes in the clustering of first or last taxon occurrences are a joint expression of evolutionary, ecological, taphonomic, and sedimentological processes. Sedimentation rates control the degree of sedimentary dilution and condensation and thus alter the time contained in a given thickness of sediment. However, it remains poorly explored quantitatively how distinct the stratigraphic patterns in the first and last occurrences can be under different deposition models with a constant thickness of accumulated sediment. Here, I present an algorithm that translates ecological or evolutionary signals between time and stratigraphic height. It is implemented for R Software as the package DAIME and complemented by tools to quantify the uncertainties associated with the construction of deposition models. By modeling the stratigraphic expression of the K/Pg extinction and an earlier extinction pulse potentially linked to Deccan volcanism on Seymour Island under varying sedimentation rates, I show that (1) clustering of last occurrences ~ 250 kyr prior to the K/Pg boundary can be equally explained by a stronger earlier extinction pulse or prolonged intervals with reduced sediment accumulation rate, but (2) when the temporal variability in sedimentation rate is known, the most plausible extinction dynamics can still be identified. The approach is applicable for any type of information transported as a part of the sedimentary record (e.g., fossils or trace elements) or data derived from it (e.g., isotope ratios and rates of morphological evolution).

INTRODUCTION

The stratigraphic record makes it possible to establish relative ages via biostratigraphy, track ecologic changes on the basis of fluctuations in absolute and relative abundance or body size of fossils, examine evolutionary patterns, or use isotope ratios from skeletal remains to reconstruct climate (e.g., Berrocoso et al. 2012; Danise and Holland 2017; Rita et al. 2019; Fan et al. 2020).

However, sedimentological parameters and the distribution of fossils can change predictably within the sequence stratigraphic architecture, making the fossil record a combined expression of sedimentological, taphonomic, evolutionary, and ecological processes (Ager 1967; Holland 2000; Holland and Patzkowsky 2015; Nawrot et al. 2018). These changes can be subdivided into the following categories:

(1) Environmental preferences of taxa: Taxa can track shifting environments through time, first and last taxon occurrences in a stratigraphic column thus do not necessarily reflect global taxon origination or extinction, but rather reflect local or regional ecologically relevant colonization or extirpation due to changing conditions such as water depth or substrate consistency (Scarponi et al. 2013; Huntley and Scarponi 2015; Nawrot et al. 2018; Dominici et al. 2018; Jarochowska et al. 2018).

(2) Temporally variable sedimentation rates and hiatuses: The sedimentary record is highly incomplete, with periods of nondeposition or removal of previously deposited sediment (Wheeler 1958; Sadler 1981; Wilkinson et al. 1991). Longer hiatuses can generate clusters of first and last occurrences above and below major hiatuses (Holland 2000) and can increase abundance of skeletal remains (Fürsich 1978; Kidwell 1985, 1986). This effect will naturally propagate to all information derived from condensed or diluted assemblages, affecting first and last occurrences, and rates of morphological evolution (Holland and Patzkowsky 2015; Scarponi et al. 2017), although empirical range endpoint clustering does not invariably correlate with hiatus durations (Peters 2006).

(3) Preservation: High sedimentation rates can correlate with high preservation potential as they bring skeletal remains outside of the taphonomically active zone fast and thereby reduce their exposure time to destructive processes close to the sediment surface (Davies et al. 1989; Brett 1995). However, whether preservation rates change systematically within depositional sequences remains poorly explored.

Wang and Marshall (2016) summarize 25 methods used to estimate the timing of taxon extinction in the fossil record on the basis of stratigraphic ranges, but only two methods explicitly incorporate environmental and sequence stratigraphic information (Holland 2003; Schueth et al. 2014). However, four out of five mass extinctions coincide with rapid changes in global sea level (Hallam 1989; Peters 2008), making them prone to the biases introduced by changes in sediment accumulation rates (Holland and Patzkowsky 2015).

The translation of stratigraphic into time-undistorted records is possible to some degree if age models constraining the bottom and the top of sections are available to provide an estimate of net sediment accumulation rate (Schwarzacher 1993; Shackleton et al. 1999; Meyers 2014; Trampush and Hayek 2017). However, the internal within-section variability in sedimentation rate, including the frequency and distribution of hiatuses, will significantly affect the reconstructed temporal signals, for example, in the number of first or last species occurrences (Amorosi et al. 2017), and the question of interest is how distinct temporal signals will be under distinct depositional models.

In this paper, I focus on the effects of variable sediment accumulation rates and hiatuses. I develop the DAIME model, which is applicable on the level of individual sections and makes it possible to (1) model how variable sediment accumulation rates and hiatuses alter the stratigraphic expression of ecological or evolutionary signals and (2) incorporate information about variable sedimentation rates and hiatuses into the analysis of these ecological or evolutionary signals observed in the stratigraphic record. Taking a deposition model (e.g., an age model or sedimentation rate) as input, this model constructs a chronostratigraphic framework to express data in terms of time instead of stratigraphic height. This model accounts for the effects of changing sediment accumulation rates while preserving the original data structure, ensuring backwards compatibility with all previously published methods that analyze data in the section. The model is implemented for R Software and available on CRAN as the package “DAIME” (Hohmann 2020). It makes it possible to transform a variety of different data types. To account for the uncertainties associated with the reconstruction of deposition models, I examine how the choice of deposition model alters the output of the DAIME model. As an example, I examine the effects of variable sediment accumulation rates on the stratigraphic expression of the K/Pg extinction and an earlier extinction pulse occurring ~ 50 m below the K/Pg boundary and how they affect the difficulty to distinguish between different intensities of the early extinction pulse. This pulse was documented in individual sections by Tobin (2017) and is potentially linked to Deccan volcanism, although analyses based on a composite section reduce the magnitude of extinction (Witts et al. 2016). To increase readability, mathematical derivations are placed in the appendices. Changing preservation and preferred habitats can be embedded in the theoretical framework underlying the model (Appendix A; Kallenberg 2017), but are not further considered in the main text.

THE DAIME MODEL

The DAIME (Deposition As Image Measure) model uses deposition models based on sedimentation rates or age models to transform information such as sample location, isotope ratios, skeletal contents of the sediment, or morphological variables from stratigraphic height to time and vice versa (Fig. 1). It is implemented for the software R (R core Team 2020) as the package “DAIME” and is available at the Comprehensive R Archive Network (CRAN) (Hohmann 2020a). Some examples are available after installation via the command vignette(‘DAIME’). The implemented transformation covers two basic data types: patterns and points.

Stratigraphic and temporal patterns simply represent rates of change in the magnitude of biotic (i.e., ecological or evolutionary) or abiotic variables measured along stratigraphic height or time. Stratigraphic patterns are sediment contents (e.g., abundance of skeletal remains, thorium concentration in the sediment, or first/last taxon occurrences per height) observed in the section and have dimension XL^{-1}, where X is the dimension of the content. Temporal patterns are inputs into the sediment per time (e.g., skeletal accumulation, thorium input, or first/last taxon occurrences per time unit) and have dimension XT^{-1} (Fig. 1). More derived rates such as morphological change per stratigraphic height can also be transformed. The transformation of temporal patterns into stratigraphic patterns and vice versa is performed by the function “patterntransform”.

Points are stratigraphic heights or points in time with dimensions L and T respectively, typically assigned to specimens or samples with negligible stratigraphic extent or events in time of negligible duration (Fig. 1). The transformation of points is performed by the function “pointtransform”. When the time of deposition or stratigraphic height of a specimen or sample is transformed, all other information associated with it (e.g., isotope measurements performed on it, including their uncertainties) that is not derived from its time of deposition or stratigraphic height remains unchanged, generating a “squeezebox effect” (Fig. 2).

Cumulative data such as the number of last occurrences found below some stratigraphic height can be transformed by recursion to the transformation of points: all data collected below a given stratigraphic height were deposited before the time of deposition of the corresponding stratigraphic height (and vice versa). In this case, the DAIME model is simply the law of superposition, applied to an age model.

For data collected in temporal or stratigraphic bins, the endpoints of bins can be transformed as points to define the corresponding bins in time or stratigraphic height. Corresponding bins in time and stratigraphic height share their data, e.g., the taxonomic richness observed in a stratigraphic bin is the taxonomic richness preserved during the corresponding temporal bin (and vice versa). Stratigraphic bins lacking data accordingly generate temporal bins lacking data. Patterns based on bins can be transformed directly using “patterntransform”. Uncertainties regarding the time of deposition or stratigraphic height of a point can be incorporated into analyses by either treating the corresponding probability density function (e.g., as temporal or stratigraphic variability in the probability of last species occurrences, summing to one) as a pattern or by transforming the cumulative distribution function as cumulative data.

Nondeposition and Erosion

The implementation of the DAIME model assumes that no fossils are preserved in times of nondeposition or erosion. When transforming stratigraphic height to time, hiatuses can be inserted into the deposition model at any height. This generates barren time intervals without transformed points or information about the temporal rate due to the destruction of information by the hiatus. Whether diastems need to be modeled explicitly depends on the depositional completeness (sensu Kowalewski and Bambach 2008) and the desired temporal resolution of the study. When transforming time into stratigraphic height, negative sediment accumulation rates or decreasing age models can be used to describe nondeposition or erosion. In this case, time intervals with net erosion will be removed, and only points and parts of temporal patterns that coincide with the remaining time intervals will be transformed into stratigraphic height.

Time Averaging and Mixing

Time-averaging is not explicitly modeled by the DAIME model. Transforming stratigraphic heights into time adds time-averaging (understood as the distribution of ages of sedimentary particles or shells at the given stratigraphic height) as uncertainty to the reconstructed time of deposition and thus limits the resolution of the transformed data. Conversely, when transforming times of deposition into stratigraphic height, mixing (understood as the distribution of burial depths of simultaneously buried sedimentary grains or shells in the depositional environment) is added as uncertainty to the resulting stratigraphic height. The addition of uncertainty can be modeled by either randomizing the transformed points or by replacing them with the probability density function describing the time-averaging/mixing in the environment of interest. Approaches that aim to unmix time averaged data (e.g., as in Tomašových et al. 2017) should be applied separately before or after the transformation. When transforming patterns, mixing and time-averaging can be modeled either based on a direct modification of patterns (e.g., via a convolution), or as a randomization of a simulated fossil record (Tomašových and Kidwell 2010; Kallenberg 2017; Hohmann 2018; Hohmann 2019a, 2019b; Appendix B; Online Supplemental File R code).

Volume of Inputs and Shell Beds

When transforming time to stratigraphic height, volume contributed by the pattern to the total sediment volume is assumed to be negligible in this implementation. When this assumption does not hold, e.g., when shells make up a considerable proportion of the sediment, the sediment accumulation rate s_{time} should be replaced by a composite sediment accumulation rate $s_{\widehat{time}} = s_{time} + v_{pat} * f_{strat}$, where v_{pat} is the volume of one unit of the pattern, f_{strat} is the temporal pattern, and s_{time} is the sedimentation rate without contribution of the pattern. The composite sediment accumulation rate incorporates the volume contributed by the pattern, and accordingly permits to model the formation of shell beds in times when shells are the dominant component of the sediment.

First and Last Taxon Occurrences

In the absence of hiatuses, first and last taxon occurrences (F/LTOs) can be transformed using the DAIME model as any other pattern. When transforming from time to stratigraphic height, the temporal succession of F/LTos can be confounded by a hiatus, as the stratigraphically lowest or highest occurrences will be declared as FTO or LTO. The number of F/LTOs in a time interval thus does not correspond to the number of F/LTos in the corresponding stratigraphic interval and the bidirectional relationship between the section and time fails, making the direct transformation of patterns and points of F/LTOs in the presence of hiatuses impossible. Explicit modeling of the fossil record can be used to circumvent this problem (Hohmann 2019a, 2019b; Appendix C; Online Supplemental File R Code). The transformation of F/LTOs from height to time in the presence of hiatuses fails for the same reasons. Due to the barren interval in time introduced by the hiatus, the timing of the F/LTO in time can only be bracketed by (1) the time of deposition of the specimen that is the F/LTO in the section and (2) the beginning/end of the hiatus.

Ratios, Percentages, and Relative Abundances

Analyzing ratios, relative abundances, and percentages of sediment contents circumvents the effect of sedimentary condensation and dilution. Although ratios or percentages are not affected by variability in sedimentation rate between stratigraphic increments, the stratigraphic heights and times where those values were measured will change when transformed between the stratigraphic and the time realm. This leads to a “squeezebox effect”, where the times or stratigraphic heights where they were measured change their position relative to each other due to sedimentary condensation or dilution while the ratios remain unchanged. This can lead to both an over- or underestimation of the volatility and the rate of change in these ratios (Fig. 2).

QUANTIFYING DIFFERENCES BETWEEN PATTERNS GENERATED BY DISTINCT SEDIMENT ACCUMULATION RATES

To account for the uncertainties associated with the construction of deposition models, I quantify how distinct deposition models alter the expression of patterns in time or stratigraphic height. When deposition models are based on different sources of information (e.g., cyclostratigraphy, radiometric ages from zircons, and biostratigraphy), this method can be applied to quantify how the differences in accuracy and precision of the geochronological constraints might alter transformed patterns by generating different intervals of condensation or dilution.

The relative entropy (RE) or Kullback-Leibler divergence is a mathematical concept linked to fundamental statements regarding the speed of convergence in probabilistic settings (Kullback and Leibler 1951; Klenke 2014). For two arbitrary patterns f_0 and f_1, it is given by

$$\Re(f_0|f_1) = \int f_1(x) - f_0(x) + f_0(x) ln\left(\frac{f_0(x)}{f_1(x)}\right) dx$$

(Hohmann 2017). The RE is a pairwise measure of distinguishability between patterns such as the temporal or stratigraphic variability in the number of last taxon occurrences. The generalized version of the RE takes into account that this dissimilarity can not only be generated by location (i.e., where last taxon occurrences are located relative to each other), but also by sample size (i.e., the total number of last taxon occurrences observed in the section). However, unknown preservation makes it difficult to distinguish whether a high or low sample size is due to the validity of a hypothesis (e.g., about low or high number of last occurrences) or due to high or low preservation potential. To account for this uncertainty, I assume that all patterns for which the RE is calculated are normalized to have an integral of one, in which case they correspond to probability density functions and the RE simplifies to

$$\Re(f_0|f_1) = \int f_0(x) \, ln\left(\frac{f_0(x)}{f_1(x)}\right) dx$$

This version of the RE does not incorporate potential differences in sample size, and is directly linked to important statistical properties (Chirikjian 2009).

One of these properties is that in a test of a pattern corresponding to the null hypothesis $H_0 = f_0$ against the alternative pattern $H_1 = f_1$, the probability of a type 2 error (not rejecting a false null hypothesis) decays exponentially as sample size n increases, with the decay constant being given by the relative entropy (Chernoff 1956; Liese and Miescke 2008, theorem 8.75):

$$\beta_n(H_0 vs. H_1) \approx exp\left(-n\Re(f_0|f_1)\right)$$

Motivated by this, I define the type 2 error half-life as the approximate number of additional observations necessary to halve the probability of a type 2 error in a test of H_0 against H_1:

$$t_{0.5}(H_0 vs. H1) = log(2)/\Re(f_0|f_1)$$

A high type 2 error half-life indicates both low distinguishability between patterns (since a large sample size is required to correctly identify them) and low efficiency of additional sampling efforts (since increasing sample size only slowly reduces the probability of a type 2 error). Conversely a low type 2 error half-life indicates high distinguishability between patterns since only a small sample size is required to correctly identify them.
Based on this, I use the symmetrized relative entropy (SRE)

$$SRE(H_0|H_1) = 0.5\left(\Re(f_0,f_1) + \Re(f_1,f_0)\right) = 0.5 * log(2)\left(1/t_{0.5}(H_0 vs. H1) + 1/t_{0.5}(H_0 vs. H1)\right)$$

as a measure of dissimilarity, where higher values reflect higher dissimilarity between the patterns f_0 and f_1 (Fig. 3).

This measure of dissimilarity can be used to quantify the relative dissimilarity between patterns generated by distinct deposition models that were used for their transformation. For this, a pattern is transformed using a set of distinct deposition models. Quantifying the dissimilarity of the resulting patterns makes it possible to measure how much the shapes of the patterns deviate relative to each other due to the choice of the deposition model. Here, low dissimilarity or a high type 2 error half-life is desirable, as they indicate that the choice of deposition model has only a weak effect on the shape of the transformed patterns and the results are robust. This dissimilarity and type 2 error can be used to compare results derived under uncertain deposition models against the assumption of a constant sediment accumulation rate. Conversely, when patterns correspond to distinct paleontological hypotheses and the deposition model is known, high dissimilarity or a low type 2 error half-life is desirable, as they permit to distinguish patterns with high certainty already based on small sample sizes.

The same underlying ideas can be used to assess the effects of incongruent sediment accumulation rates on the transformation of points, e.g., after transforming a point (and the uncertainty associated with it) using different deposition models, the variability of the results is an indicator of their robustness under the deposition models used for the transformation. The mathematical background for this section is given in Appendix D (Sanov 1958; Meester 2008; Chirikjian 2009; Klenke 2014; Kallenberg 2017).

EXAMPLE: THE K/PG BOUNDARY ON SEYMOUR ISLAND, ANTARCTICA

Using these measures of dissimilarity based on the relative entropy, I examine the effects of conflicting deposition models on the stratigraphic expression of the K/Pg extinction and the recognition of an earlier extinction pulse potentially linked to Deccan volcanism. For this, I use data from Seymour Island, Antarctica, a well-studied section that consists of Late Cretaceous to early Paleogene marine sand to siltstones that are rich in macrofossils documenting biotic and abiotic changes before and at the K/Pg boundary (Macellari 1986, 1988a, 1988b; Zinsmeister et al. 1989; Zinsmeister 1998; Witts et al. 2016; Petersen et al. 2016; Linzmeier et al. 2020).

The influence of the Deccan traps on the K/Pg extinction has been discussed for a long time (Officer and Drake 1985; Keller 1988). One pulse of Deccan volcanism predates the K/Pg boundary (Schoene et al. 2019), leading to a discussion whether volcanism and the associated climate change caused elevated extinction rates before the K/Pg boundary (Tobin et al. 2012; Petersen et al. 2016).

The location of the iridium layer associated with the asteroid impact at the K/Pg boundary first proposed by Alvarez et al. (1980) is well known on Seymour Island (Elliot et al. 1994). The abrupt nature of this event in combination with the assumption that fossils found on Seymour Island have uniform recovery potential (Wang et al. 2009) lead to a frequent usage of data from this section to demonstrate the performance of statistical methods that derive information about extinction events (e.g., Strauss and Sadler 1989; Springer 1990; Marshall 1995; Solow and Smith 2000; Wang et al. 2012; Tobin 2017). On one hand, the assumption of a uniform recovery potential is challenged by the interpretation by Macellari (1988b) of a relative sea-level stillstand at the K/Pg boundary and a bioturbated horizon approximately 50 m below, interpreted as corresponding to a maximum flooding interval and the transition from “transgressive” facies to “regressive” facies (Appendix E). On the other hand, Crame et al. (2004) and Tobin (2017) did not detect any condensation at this level and Witts et al. (2016) age model informed by magnetostratigraphic constraints does not show any significant decline in sedimentation rate.

Other authors report the presence of hardgrounds below the K/Pg boundary (Crame et al. 2004) as well as lag deposits (Zinsmeister 1998), and increased diversity and more offshore assemblages in dinocysts (Elliot et al. 1994) right at the K/Pg boundary. Section A from Witts et al. (2016) further shows a simultaneous spike in the number of first and last taxon occurrences correlating with the maximum flooding interval proposed by Macellari (1988b) and identified by Tobin (2017) to represent an earlier extinction event. Such spike can also indicate condensation or a hiatus (Kidwell 1985; Holland 2000) (Fig. 4), although true changes in extinction or origination can be also coupled with changes in sedimentation rate.

I examine how the condensation interval prior to the K/Pg boundary and a decreased sedimentation rate at the K/Pg boundary proposed by Macellari (1988b) (1) alters the stratigraphic expression of the extinction dynamics before and at the K/Pg boundary compared to constant sediment accumulation and (2) how this affects the recognition of the early extinction pulse.

Deposition Models

Stratigraphic height is based on the composite section from Witts et al. (2016). All deposition models are constrained by (1) the K/Pg boundary with stratigraphic height 1007.5 m (Witts et al. 2016, supplemental material) and age 66.04 Ma (Renne et al. 2013) and (2) the stratigraphic height 934.4 m with an age of 66.40 Ma based on magnetostratigraphy (Tobin et al. 2012; Gradstein et al. 2012). This corresponds to an average sedimentation rate of 209.5 m per Myr, or ~ 0.02 cm/y. The duration of this stratigraphic interval is thus ~ 400 kyr.

To generate a set of deposition models that match Macellari’s (1988b) interpretation, I defined a parametric deposition model with the condition of having a low sediment accumulation rate at 959.5 m, the stratigraphic height correlated to the maximum flooding interval proposed by Macellari (1988b). Model parameters are (1) time until the end of the low sedimentation interval (measured from the oldest point of the examined stratigraphic interval); (2) sediment accumulation rate at the low sedimentation interval; (3) sediment accumulation rate after the low sedimentation interval; and (4) sediment accumulation rate at the K/Pg boundary. For the parameters, I used a 10 or 100-fold decrease relative to the average sediment accumulation rate as low or very low sediment accumulation rate. Durations of the low sedimentation interval range from very short (0.05 Myr) to short (0.1 Myr), intermediate (0.15 Myr), and long (0.2 Myr) relative to the age of the oldest point of the examined interval. By taking all possible combinations of (1) a very short, short, intermediate, and long duration of the low sedimentation interval; (2) low or very low sediment accumulation rate at the low sedimentation interval; (3) low or average sediment accumulation rate after the low sedimentation interval; and (4) low or average sediment accumulation rate at the K/Pg boundary, 32 deposition models were created. As the 33rd deposition model and reference point, the “null hypothesis” of a constant sediment accumulation rate used by Witts et al. (2016) was added (Fig. 5, Online Supplemental File Table 1).

Extinction Models

As the pre-K/Pg extinction pulse, I use the extinction interval identified by Tobin (2017) in the data from Witts et al. (2016). For each of the 33 deposition models, it was transformed into time using the function “pointtransform” where it was combined with a spike in extinction rate at the K/Pg boundary to form five different extinction hypotheses, in which the relative contribution of the early extinction interval to the total number of extinctions ranges from none (0%) to weak (10%), intermediate (20%), strong (30%), to very strong (40%). From these extinction rates, the patterns of last taxon occurrences in time (i.e., ages of the last preserved specimens of individual species) were derived based on the convolution procedure described in Hohmann (2018). For a given extinction rate, it determines the offset between extinctions and last occurrences based on the frequency of specimens in time. This generates the characteristic backwards smearing of the Signor-Lipps effect (Signor and Lipps 1982) that becomes more pronounced when specimen frequency is low (Fig. 6). The procedure assumes specimen frequency is (1) independent of extinction; (2) constant through time; and (3) identical for all taxa.

Using the function “patterntransform”, the temporal patterns of last taxon occurrences were transformed into stratigraphic patterns of last taxon occurrences (Fig. 7). Note that since the stratigraphic height of the extinction interval is fixed, each deposition model will generate a different absolute age of the extinction pulse. To account for the effect of specimen frequency on the recognition of extinctions (Signor and Lipps 1982), this procedure was repeated with specimen frequencies ranging from 10 to 140 specimens per Myr in the convolution procedure. Under constant sedimentation rate, this corresponds to a specimen abundance in the section ranging from finding one fossil per 20 meters to finding two fossils per three meters.

In total, this procedure yields a collection of last taxon occurrences in the section as a function of the deposition model, relative contribution of the early extinction pulse, and specimen frequency.

Analysis

For fixed specimen frequencies, I determined RE, SRE, and type 2 error half-life between pairs of last taxon occurrences transformed by different deposition models and with different contributions of the early extinction pulse. Both for a fixed contribution of the early extinction pulse and all contributions combined, I used a matrix containing the SREs as distance matrix for a non-metric multidimensional distance scaling (NMDS) using the isoMDS function of the R package MASS (Kruskal 1964a, 1964b; Venables and Ripley 2002)

Results

Generated by the low sedimentation interval, last taxon occurrences in the section display a spike similar to the one observed in section A from Witts et al. (2016). When sedimentation rate at the K/Pg boundary is low, last taxon occurrences are closer to the boundary and more frequent, accentuating the extinction (Fig. 7).

For any deposition model, type 2 error half-life between pairs of last taxon occurrences generated by different contributions of the early extinction pulse is almost constant for more than 40 specimens per Myr and grows exponentially for lower values, showing that moderately abundant taxa are as suitable as very abundant taxa to distinguish the extinction hypothesis (Fig. 8A). As the intensity of the early extinction pulse increases from none to strong, type 2 error half-life increases by a factor of more than three, implying that it is a lot easier to decide whether an early extinction pulse is present (none vs. weak) than to assess its exact intensity (e.g., strong vs. very strong) (Fig. 8A). Generally type 2 error half-lives are high, indicating that distinguishing different intensities of early extinction pulses via the extinctions they generate requires datasets with high taxonomic richness.

The deposition model used for the transformation of the extinction hypotheses show only a minor influence on the type 2 error half-life (Fig. 8B). When the deposition model is known, the ability to differentiate between different extinction dynamics is thus independent of the properties of the deposition model.

For fixed contributions of the early extinction pulse, the NMDS between the last taxon occurrences in stratigraphic height shows two separate lines, each corresponding to a different sediment accumulation rate at the K/Pg boundary (Fig. 9). The position of deposition models within these lines is determined by the duration of the low sedimentation interval (Fig. 9). Sediment accumulation rates at and after this interval show only little influence on the position of deposition models in the ordination. The null model of a constant sediment accumulation rate is located close to the deposition models with average sediment accumulation rate (i.e., 0.02 cm/a) at the K/Pg extinction and a short duration of the low sedimentation interval (i.e., it ends at 66.3 Ma). Sediment accumulation rate at the K/Pg boundary is thus the strongest control on the stratigraphic expression of the extinction scenarios, followed by duration of the low sedimentation interval.

The NMDS of different contributions of the early extinction pulse as well as varying durations of the low sedimentation interval and sedimentation rates at the K/Pg boundary confirms these results (Fig. 10). Different contributions of the early pulse form parallel lines because the dissimilarity does not depend on the deposition model used (Fig. 8B), and these lines are closer to each other as the contribution of the early pulse increases because stronger contributions of the early pulse are harder to distinguish from each other (Fig. 8A). As in Figure 9, low or average sedimentation rates at the K/Pg boundary are well separated lines that are internally sorted according to the duration of the low sedimentation interval.

When the sedimentation rate at the K/Pg boundary is low (i.e., 0.002 cm/a), dissimilarity of the distribution of last taxon occurrences is equally controlled by (1) the duration of the low sedimentation interval and (2) the intensity of the early extinction pulse. Deviations from an expected pattern can accordingly be attributed both to a stronger or weaker influence of the early extinction pulse or to a longer or shorter interval with low sedimentation rates (Fig. 10).

Without the constraints on deposition models, the variability in the number of last taxon occurrences observed in the section are overdetermined as they can be generated by either (1) a deposition model and suitably chosen number of last taxon occurrences that vary in time or (2) last taxon occurrences in time and a suitably chosen deposition model with variable sedimentation rate (using the function “patterntodepositonmodel”). In the latter case, the generated deposition models will roughly match Macellari’s interpretation if last occurrences in the section have a higher contribution of the early extinction pulse than the last occurrences on the section, however they will in general not be encompassed by the 33 deposition models used in this example. As an example, the deposition model transforming last taxon occurrences generated by an extinction scenario with no early extinction pulse into the last taxon occurrences resembling an intermediate contribution of the early extinction pulse (Fig. 7) is given in Figure 5. Inferences about the extinction dynamics thus necessarily require knowledge about temporal variability in sedimentation rate.

MATHEMATICAL BACKGROUND

The instantaneous sediment accumulation rate $s_{time}(t)$ describes the sediment accumulated per time unit. By tracing the amount of sediment accumulated up to time t, it defines an age model H_{strat} via

$$H_{strat}(t) = \int^{t} s_{time}(x)dx$$

where $H_{strat}(t)$ is the stratigraphic height deposited at time t. Its inverse function is given by

$$T_{dep}(h) = \int^{h} 1/s_{strat}(x)dx$$

and assigns the stratigraphic height h its time of deposition $T_{dep}(h)$ (Callahan 2010, theorem 5.2). Here, $s_{strat}(x)$ is the instantaneous sediment accumulation rate in the section, assigning the stratigraphic height x the instantaneous sediment accumulation rate with which it was deposited, and $1/s_{strat}(x)$ is the inverse instantaneous sediment accumulation rate, quantifying the time required to deposit one unit of sediment at the stratigraphic height x. The age models H_{strat}, T_{dep} and the sediment accumulation rates $s_{time}, s_{strat}, 1/s_{strat}$ can be transformed into each other via differentiation, integration, and inversion and are thus equivalent representations of the same deposition model (Appendix F). In the implementation, the preserved net sedimentation rate can be obtained by taking the difference quotients of H_{strat} after time intervals with erosion were removed.

The bidirectional relation between points in time and the section extends to bins: A stratigraphic bin $B_{strat} = [h_1, h_2]$ is connected with the time bin $B_{time} = [T_{dep}(h_1), T_{dep}(h_2)]$ of its deposition, and a time bin $B_{time} = [t_1, t_2]$ is connected with the stratigraphic bin $B_{strat} = [H_{strat}(t_1), H_{strat}(t_2)]$ that was formed during this time bin (Fig. 1). The DAIME model assumes that that preservation is constant. It is known that taphonomic conditions change along depositional gradients (Brett 1995); see Appendix A for how changes in preservation rate can be incorporated into analyses. To simplify notation, I omit proportionality constants introduced by the loss of a fixed, but unknown proportion of the input into the sediment due to constant preservation.

Based on the assumption of constant preservation, the bidirectional relation between bins expands to inputs and contents, forming the core idea of the DAIME model: any input V_{time} into the sediment during the time bin $[t_1, t_2]$ is equivalent to the observed content V_{strat} in the sediment in the corresponding bin $[H_{strat}(t_1), H_{strat}(t_2)]$ in the section, and they have identical dimensions. Conversely any content of the sediment V_{strat} in the bin $[h_1, h_2]$ in the section is equivalent to the input into the sediment V_{time} during the time bin $[T_{dep}(h_1), T_{dep}(h_2)]$ during which it was deposited, and they have identical dimensions (Fig. 1).

Taking V_{strat} and V_{time} as measures in the mathematical sense of generalized volumes, the above relations describe how the two measures are transformed into each other by the means of a deposition model. This transformation is called as an image measure or pushforward measure and serves as the namesake of the DAIME (Deposition As Image MEasure) model (Klenke 2014, definition 1.98). The image measure formalizes how volumes behave under coordinate transformations such as the transformation between time and height. This is achieved by assigning a set after coordinate transformation (the image) the same volume as its equivalent set (the preimage) before the transformation.

The input V_{time} or content V_{strat} with dimension X can alternatively be described using an input rate f_{time} or content rate f_{strat}, corresponding to the temporal pattern with dimension X/T and the stratigraphic pattern with dimensions X/L respectively.
Based on the connection between input and content as image measures of each other, explicit representations of the temporal and stratigraphic patterns can be given (Klenke

2014, theorem 1.101) (Fig. 1). The stratigraphic pattern f_{strat} generated by the deposition model T_{dep} and the temporal pattern f_{time} is given by

$$f_{strat}(h) = f_{time}\left(T_{dep}(h)\right)/s_{time}\left(T_{dep}(h)\right)$$

Conversely, the temporal pattern f_{time} generated by a stratigraphic pattern f_{strat} in combination with a deposition model H_{strat} is given by

$$f_{time}(t) = f_{strat}\big(H_{strat}(t)\big)s_{strat}\big(H_{strat}(t)\big)$$

These relations make it possible to directly transform stratigraphic patterns into temporal patterns and vice versa (Appendix G).

DISCUSSION

I have developed the DAIME model, describing how changing sediment accumulation rates and hiatuses condense and dilute any type of information that is conveyed as part of the sedimentary rock record (section "The DAIME Model"). DAIME permits transforming a variety of data types such as (first/last) taxon occurrences, isotope ratios, trace element contents, and rates of morphological evolution between time and stratigraphic height on the basis of independently derived deposition models. Using this as a data preprocessing tool for any stratigraphy-based statistical method makes it possible to account for the effects changing sediment accumulation rates and hiatuses in the analysis.

Constructing Deposition Models

Age models have been published for many sections spanning major extinction events (e.g., Torfstein et al. 2010 for the PETM; Deenen et al. 2010 for the end Triassic; Burgess et al. 2014 for the end Permian; Hull et al. 2020 for the end-Cretaceous). Absolute ages at given stratigraphic heights in a section provide limits on the maximum duration of deposition and hiatuses as well as on the volume of deposition. However, even in the absence of absolute ages, the effects of varying sediment accumulation rates can be approximated quantitatively and compared using an auxiliary relative age model ranging from 0 (lowest part of the section) to 1 (highest part of the section), an approach that has been successfully applied to a Silurian carbonate platform (Jarochowska et al. 2020). Both approaches can be refined using sequence stratigraphic interpretations to inform about relative changes in sediment accumulation rates, characterizing intervals with higher or lower sediment accumulation rates, identifying gradients of sediment accumulation rates, and putting constraints of the duration and location of hiatuses (Galloway and Williams 1991; Amorosi et al. 2020).

Using the function "patterntodepositionmodel" from the DAIME package, geochemical and palynological data can be turned into deposition models by combining assumptions of input through time (e.g., thorium or pollen; Adams and Weaver 1958) with observed stratigraphic patterns to derive the deposition model that dilutes/condenses one into the other. A special case of this approach is applied in Holocene environments, where the dilution and decay of a constant support of ^{210}Pb is used to construct age models and sediment accumulation rates (Appleby and Oldfield 1978; periodic flux model sensu Sanchez-Cabeza et al. 2000; constant flux model sensu Sanchez-Cabeza and Ruiz-Fernández 2012).

Uncertainties associated with estimated deposition models or incongruities between different deposition models can be addressed with the methods described in the section "Quantifying the Effects of Incongruent Sediment Accumulation Rates". They provide both an absolute and a relative measure of (dis)similarity for sets of deposition models, and can accordingly be used to measure to what extent patterns and point estimates change relative to each other based on the choice of the deposition model. This makes it possible to construct a range of temporal patterns that are potential explanations for the patterns observed in the section, given the uncertainties about the knowledge of the depositional environment such as duration of hiatuses. Most importantly, this approach offers the opportunity to compare the effect of the assumption of a constant sediment accumulation rate against any set of other deposition models available.

DATA ACCESSIBILITY STATEMENT

All data generated for the examples is available via the doi 10.17605/OSF.IO/AEFNZ, code used for this manuscript is available in the electronic supplementary materials. The interactive web application “The Shellbed Condensator” by Hohmann and Jarochowska (2021) provides a visualization of the DAIME model.

ACKNOWLEDGMENTS

I would like to thank Emilia Jarochowska for her encouragement and detailed feedback during the development of this project. The manuscript has greatly profited from comments by Steven Holland, Rafal Nawrot, Mark Patzkowsky, Peter Sadler, Adam Tomašových, and Martin Zuschin.

SUPPLEMENTAL MATERIAL

Data are available from the PALAIOS Data Archive: https://www.sepm.org/supplemental-materials.

REFERENCES

Adams, J.A.S. and Weaver, C.E., 1958, Thorium-to-uranium ratios as indicators of sedimentary processes: example of concept of geochemical facies: AAPG Bulletin, v. 42, p. 387–430.

Ager, D.V., 1967, Brachiopod palaeoecology: Earth-Science Reviews, v. 3, p. 157–179.

Alvarez, L.W., Alvarez, W., Asaro, F., and Michel, H.V., 1980, Extraterrestrial cause for the Cretaceous–Tertiary extinction: Science, v. 208, p. 1095–1108.

Appleby, P.G. and Oldfield, F., 1978, The calculation of lead-210 dates assuming a constant rate of supply of unsupported 210Pb to the sediment: Catena, v. 5, p. 1–8.

Amorosi, A., Bohacs, K.M., Bruno, L., Campo, B., and Drexler, T.M., 2017, How close is geological thought to reality? The concept of time as revealed by the sequence stratigraphy of the Late Quaternary record, *in* B. Hart, N.C. Rosen, D. West, A. D’Agostino, C. Messina, M. Hoffman, and R. Wild (eds.), Sequence Stratigraphy: The Future Defined: SEPM Gulf Coast Section Publications, v. 36, p. 47–86, doi: 10.5724/gcs.17.

Brett, C.E., 1995, Sequence stratigraphy, biostratigraphy, and taphonomy in shallow marine environments: PALAIOS, v. 10, p. 597–616.

Berrocoso, À.J., Huber, B.T., MacLeod, K.G., Petrizzo, M.R., Lees, J.A., Wendler, I., Coxall, H., Mweneinda, A.K., Falzoni, F., Birch, H., Singano, J.M., Haynes, S., Cotton, L., Wendler, J., Bown, P.R., Robinson, S.A., and Gould, J., 2012, Lithostratigraphy, biostratigraphy and chemostratigraphy of Upper Cretaceous and Paleogene sediments from southern Tanzania: Tanzania Drilling Project Sites 27–35: Journal of African Earth Sciences, v. 70, p. 36–57.

Burgess, S.D., Bowring, S., and Shen, S., 2014, High-precision timeline for Earth’s most severe extinction: Proceedings of the National Academy of Sciences, v. 111, p. 3316–3321.

Callahan, J.J., 2010, Advanced Calculus: A Geometric View: Springer, New York, 542 p.

Chernoff, H., 1956, Large-sample theory: parametric case: The Annals of Mathematical Statistics, v. 27, p. 1–22.

CHIRIKJIAN, G., 2009, Stochastic Models, Information Theory, and Lie Groups, Volume 1: Classical Results and Geometric Methods: Birkhäuser, Boston, 405 p.

CRAME, J., FRANCIS, J., CANTRILL, D., AND PIRRIE, D., 2004, Maastrichtian stratigraphy of Antarctica: Cretaceous Research, v. 25, p. 411–423.

DANISE, S. AND HOLLAND, S.M., 2017, Faunal response to sea-level and climate change in a short-lived seaway: Jurassic of the Western Interior, USA: Palaeontology, v. 60, p. 213–232.

DAVIES, D.J., POWELL, E.N., AND STANTON, R.J., 1989, Relative rates of shell dissolution and net sediment accumulation—a commentary: can shell beds form by the gradual accumulation of biogenic debris on the sea floor?: Lethaia, v. 22, p. 207–212.

DEENEN, M.H.L., RUHL, M., BONIS, N.R., KRIJGSMAN, W., KUERSCHNER, W.M., REITSMA, M., AND VAN BERGEN, M.J., 2010, A new chronology for the end-Triassic mass extinction: Earth and Planetary Science Letters, v. 291, p. 113–125.

DOMINICI, S., DANISE, S., AND BENVENUTI, M., 2018, Pliocene stratigraphic paleobiology in Tuscany and the fossil record of marine megafauna: Earth-Science Reviews, v. 176, p. 277–310.

ELLIOT, D.H., ASKIN, R.A., KYTE, F.T., AND ZINSMEISTER, W.J., 1994, Iridium and dinocysts at the Cretaceous–Tertiary boundary on Seymour Island, Antarctica: implications for the K-T event: Geology, v. 22, p. 675–678.

FAN, J.-X., SHEN, S.-Z., ERWIN, D.H., SADLER, P.M., MACLEOD, N., CHENG, Q.-M., HOU, X.-D., YANG, J., WANG, X.-D.,WANG, Y., ZHANG, H., CHEN, X., LI, G.-X., ZHANG, Y.-C., SHI, Y.-K., YUAN, D.-X. CHEN, Q., ZHANG, L.-N., LI, C., AND ZHAO, Y.-Y., 2020, A high-resolution summary of Cambrian to Early Triassic marine invertebrate biodiversity: Science, v. 367, p. 272–277.

FÜRSICH, F.T., 1978, The influence of faunal condensation and mixing on the preservation of fossil benthic communities: Lethaia, v. 11, p. 243–250.

GALLOWAY, W.E. AND WILLIAMS, T.A., 1991, Sediment accumulation rates in time and space: Paleogene genetic stratigraphic sequences of the northwestern Gulf of Mexico basin: Geology, v. 19, p. 986–989.

GRADSTEIN, F.M., OGG, J.G., SCHMITZ, M., AND OGG, G., 2012, The Geologic Time Scale: Elsevier, Boston, 1176 pages.

HALLAM, A., 1989, The case for sea-level change as a dominant causal factor in mass extinction of marine invertebrates: Philosophical Transactions of the Royal Society of London B, Biological Sciences, v. 325, p. 437–455.

HOHMANN, N., 2017, Testing hypotheses on population dynamics: a test for the inhomogeneous Poisson point process model: Preprint, bioRxiv 234948, doi: 10.1101/234948.

HOHMANN, N., 2018, Reversing time averaging and reconstructing extinction rates with approaches from image processing: Preprint, bioRxiv 408864, doi: 10.1101/408864.

HOHMANN, N., 2019a, Conditional densities and simulations of inhomogeneous Poisson Point processes: Preprint, ArXiv:1901.10754.

HOHMANN, N., 2019b, R Package IPPP: Comprehensive R Archive Network (CRAN), doi: 10.5281/zenodo.3542336.

HOHMANN, N., 2020, R package DAIME: Comprehensive R Archive Network (CRAN), doi: 10.5281/zenodo.3702552.

HOHMANN, N. AND JAROCHOWSKA, E., 2021, The Shellbed Condensator, https://stratigraphicpaleobiology.shinyapps.io/shellbed_condensator/. Checked February 2021.

HOLLAND, S.M., 2000, The quality of the fossil record: a sequence stratigraphic perspective: Paleobiology, v. 26, p. 148–168.

Holland, S.M., 2003, Confidence limits on fossil ranges that account for facies changes: Paleobiology, v. 29, p. 468–479.

Holland, S.M. and Patzkowsky, M.E., 2015, The stratigraphy of mass extinction: Palaeontology, v. 58, p. 903–924.

Hull, P.M., Bornemann, A., Penman, D.E., Henehan, M.J., Norris, R.D., Wilson, P.A., Blum, P., Alegret, L., Batenburg, S.J., Bown, P.R., Bralower, T.J., Cournede, C., Deutsch, A., Donner, B., Friedrich, O., Jehle, S., Kim, H., Kroon, D., Lippert, P.C., Loroch, D., Moebius, I., Moriya, K., Peppe, D.J., Ravizza, G.E., Röhl, U., Schueth, J.D., Sepúlveda, J., Sexton, P.F., Sibert, E.C., Śliwińska, K.K., Summons, R.E., Thomas, E., Westerhold, T., Whiteside, J.H., Yamaguchi, T., and Zachos, J.C., 2020, On impact and volcanism across the Cretaceous–Paleogene boundary: Science, v. 367, p. 266–272.

Huntley, J.W. and Scarponi, D., 2015, Geographic variation of parasitic and predatory traces on mollusks in the northern Adriatic Sea, Italy: implications for the stratigraphic paleobiology of biotic interactions: Paleobiology, v. 41, p. 134–153.

Jarochowska, E., Nohl, T., Grohganz, M., Hohmann, N., Vandenbroucke, T.R.A., and Munnecke, A., 2020, Reconstructing depositional rates and their effect on paleoenvironmental proxies: the case of the Lau carbon isotope excursion in Gotland, Sweden: Paleoceanography and Paleoclimatology, v. 35, e2020PA003979, doi: 10.1029/2020PA003979.

Jarochowska, E., Ray, D.C., Röstel, P., Worton, G., and Munnecke, A., 2018, Harnessing stratigraphic bias at the section scale: conodont diversity in the Homerian (Silurian) of the Midland platform, England: Palaeontology, v. 61, p. 57–76.

Kallenberg, O., 2017, Random Measures: Springer, New York, 708 p.

Keller, G., 1988, Extinction, survivorship and evolution of planktic foraminifera across the Cretaceous/Tertiary boundary at El Kef, Tunisia: Marine Micropaleontology, v. 13, p. 239–263.

Kidwell, S.M., 1985, Palaeobiological and sedimentological implications of fossil concentrations: Nature, v. 318, p. 457–460.

Kidwell, S.M., 1986, Models for fossil concentrations: paleobiologic implications: Paleobiology, v. 12, p. 6–24.

Klenke, A., 2014, Probability Theory, A Comprehensive Course: Springer, London, 650 p.

Kowalewski, M. and Bambach, R.K., 2008, The limits of paleontological resolution, *in* P.J. Harries (ed.), High-Resolution Approaches in Stratigraphic Paleontology: Springer, Dodrecht, p. 1–48.

Kruskal, J.B., 1964a, Multidimensional scaling by optimizing goodness of fit to a nonmetric hypothesis: Psychometrika, v. 29, p. 1–27.

Kruskal, J.B., 1964b, Nonmetric multidimensional scaling: a numerical method: Psychometrika, v. 29, p. 115–129.

Kullback, S. and Leibler, R.A., 1951, On information and sufficiency: Annals of Mathematical Statistics, v. 22, p. 79–86.

Liese, F. and Miescke, K.-J., 2008, Statistical Decision Theory: Springer, New York, 694 p.

Linzmeier, B.J., Jacobson, A.D., Sageman, B.B., Hurtgen, M.T., Ankney, M.E., Petersen, S.V., Tobin, T.S., Kitch, G.D., and Wang, J., 2020, Calcium isotope evidence for environmental variability before and across the Cretaceous-Paleogene mass extinction: Geology, v. 48, p. 34–38.

Macellari, C.E., 1986, Late Campanian–Maastrichtian ammonite fauna from Seymour Island (Antarctic Peninsula): Paleontological Society Memoir, v. 18, p.1–55.

Macellari, C.E., 1988a, Bivalvia (Mollusca) from Seymour Island, Antarctic Peninsula: Geology and Paleontology of Seymour Island, Antarctic Peninsula, v. 169, p. 253–284.

Macellari, C.E., 1988b, Stratigraphy, sedimentology, and paleoecology of Upper Cretaceous/Paleocene shelf-deltaic sediments of Seymour Island: Geological Society of America Memoir, v. 169, p. 25–53.

Marshall, C.R., 1995, Distinguishing between sudden and gradual extinctions in the fossil record: predicting the position of the Cretaceous–Tertiary iridium anomaly using the ammonite fossil record on Seymour Island, Antarctica: Geology, v. 23, p. 731–734.

Meester, R., 2008, A Natural Introduction to Probability Theory: Birkhäuser, Basel, 208 p.

Meyers, S.R., 2014, R package Astrochron: Comprehensive R Archive Network (CRAN), https://cran.r-project.org/package=astrochron.

Nawrot, R., Scarponi, D., Azzarone, M., Dexter, T.A., Kusnerik, K.M., Wittmer, J.M., Amorosi, A., and Kowalewski, M., 2018, Stratigraphic signatures of mass extinctions: ecological and sedimentary determinants: Proceedings of the Royal Society B, v. 285, p. 20181191.

Officer, C.B. and Drake, C.L., 1985, Terminal Cretaceous environmental events: Science, v. 227, p. 1161–1167.

Peters, S.E., 2006, Genus extinction, origination, and the durations of sedimentary hiatuses: Paleobiology, v. 32, p. 387–407.

Peters, S.E., 2008, Environmental determinants of extinction selectivity in the fossil record: Nature, v. 454, p. 626–629.

Petersen, S.V., Dutton, A., and Lohmann, K.C., 2016, End-Cretaceous extinction in Antarctica linked to both Deccan volcanism and meteorite impact via climate change: Nature Communications; v. 7, p. 12079, doi: 10.1038/ncomms12079.

R Core Team, 2020, R: A language and environment for statistical computing: R Foundation for Statistical Computing, Vienna, Austria, https://www.r-project.org/.

Renne, P.R., Deino, A.L., Hilgen, F.J., Kuiper, K.F., Mark, D.F., Mitchell III, W.S., Morgan, L.E., Mundil, R., and Smit, J., 2013, Time scales of critical events around the Cretaceous–Paleogene boundary: Science, v. 339, p. 684–687.

Rita, P., Nätscher, P., Duarte, L.V., Weis, R., and De Baets, K., 2019, Mechanisms and drivers of belemnite body-size dynamics across the Pliensbachian–Toarcian crisis: Royal Society Open Science, v. 6, p. 190494, doi: 10.1098/rsos.190494.

Sadler, P.M., 1981, Sediment accumulation rates and the completeness of stratigraphic sections: The Journal of Geology, v. 89, p. 569–584.

Sanchez-Cabeza, J.A., Ani-Ragolta, I., and Masque, P., 2000, Some considerations of the 210Pb constant rate of supply (CRS) dating model: Limnology and Oceanography, v. 45, p. 990–995.

Sanchez-Cabeza, J.A. and Ruiz-Fernández, A.C., 2012, 210Pb sediment radiochronology: an integrated formulation and classification of dating models: Geochimica et Cosmochimica Acta, v. 82, p. 183–200.

Sanov, I.N., 1958, On the Probability of Large Deviations of Random Variables: United States Air Force, Office of Scientific Research, http://www.lib.ncsu.edu/resolver/1840.4/2119.

Scarponi, D., Azzarone, M., Kusnerik, K., Amorosi, A., Bohacs, K.M., Drexler, T.M., and Kowalewski, M., 2017, Systematic vertical and lateral changes in quality and time resolution of the macrofossil record: insights from Holocene transgressive deposits, Po coastal plain, Italy: Marine and Petroleum Geology, v. 87, p. 128–136.

Scarponi, D., Kaufman, D., Amorosi, A., and Kowalewski, M., 2013, Sequence stratigraphy and the resolution of the fossil record: Geology, v. 41, p. 239–242.

Schoene, B., Eddy, M.P., Samperton, K.M., Keller, C.B., Keller, G., Adatte, T., and Khadri, S.F.R., 2019, U-Pb constraints on pulsed eruption of the Deccan Traps across the end-Cretaceous mass extinction: Science, v. 363, p. 862–866.

Schueth, J.D., Keller, K., Bralower, T.J., and Patzkowsky, M.E., 2014, The Probable Datum Method (PDM): a technique for estimating the age of origination or extinction of nannoplankton: Paleobiology, v. 40, p. 541–559.

Schwarzacher, W., 1993, Milankovitch cycles in the pre-Pleistocene stratigraphic record: a review: Geological Society Special Publications, v. 70, p. 187–194.

Shackleton, N.J., Crowhurst, S.J., Weedon, G.P., and Laskar, J., 1999, Astronomical calibration of Oligocene–Miocene time: Philosophical Transactions of the Royal Society of London, Series A, Mathematical, Physical and Engineering Sciences, v. 357, p. 1907–1929.

Shaw, A.B., 1964, Time in Stratigraphy: McGraw-Hill, New York, 365 p.

Signor, P.W. and Lipps, J.H., 1982, Sampling bias, gradual extinction patterns, and catastrophes in the fossil record, *in* L.T. Silver and P.H. Schultz (eds.), Geological Implications of Impacts of Large Asteroids and Comets on the Earth: Geological Society of America Special Publication 190, p. 291–296.

Solow, A.R. and Smith, W.K., 2000, Testing for a mass extinction without selecting taxa: Paleobiology, v. 26, p. 647–650.

Springer, M.S., 1990, The effect of random range truncations on patterns of evolution in the fossil record: Paleobiology, v. 16, p. 512–520.

Strauss, D. and Sadler, P.M., 1989, Classical confidence intervals and Bayesian probability estimates for ends of local taxon ranges: Mathematical Geology, v. 21, p. 411–427.

Tobin, T.S., 2017, Recognition of a likely two phased extinction at the K-Pg boundary in Antarctica: Scientific Reports, v. 7, article 16317, doi: 10.1038/s41598-017-16515-x.

Tobin, T.S., Ward, P.D., Steig, E.J., Olivero, E.B., Hilburn, I.A., Mitchell, R.N., Diamond, M.R., Raub, T.D., and Kirschvink, J.L., 2012, Extinction patterns, $\delta^{18}O$ trends, and magnetostratigraphy from a southern high-latitude Cretaceous–Paleogene section: links with Deccan volcanism: Palaeogeography, Palaeoclimatology, Palaeoecology, v. 350, p. 180–188.

Tomašových, A., Gallmetzer, I., Haselmair, A., Kaufmann, D.S., Vidović, J., and Zuschin, M., 2017, Stratigraphic unmixing reveals repeated hypoxia events over the past 500 yr in the northern Adriatic Sea: Geology, v. 45, p. 363–366.

Tomašových, A. and Kidwell, S.M., 2010, The effects of temporal resolution on species turnover and on testing metacommunity models: The American Naturalist, v. 175, p. 587–606.

Torfstein, A., Winckler, G., and Tripati, A., 2010, Productivity feedback did not terminate the Paleocene–Eocene Thermal Maximum (PETM): Climate of the Past, v. 6, p. 265–272.

Trampush, S.M. and Hajek, E.A., 2017, Preserving proxy records in dynamic landscapes: modeling and examples from the Paleocene–Eocene Thermal Maximum: Geology, v. 45, p. 967–970.

Venables, W.N. and Ripley, B.D., 2002, Modern Applied Statistics with S: Springer, New York, 510 p.

Wang, S.C., Chudzicki, D.J., and Everson, P.J., 2009, Optimal estimators of the position of a mass extinction when recovery potential is uniform: Paleobiology, v. 35, p. 447–459.

Wang, S.C. and Marshall, C.R., 2016, Estimating times of extinction in the fossil record: Biology Letters, v. 12, article 20150989, doi: 10.1098/rsbl.2015.0989.

Wang, S.C., Zimmerman, A.E., McVeigh, B.S., Everson, P.J., and Wong, H., 2012, Confidence intervals for the duration of a mass extinction: Paleobiology, v. 38, p. 265–277.

Wheeler, H.E., 1958, Time-stratigraphy: AAPG Bulletin, v. 42, p. 1047–1063.

Wilkinson, B.H., Opdyke, B.N., and Algeo, T.J., 1991, Time partitioning in cratonic carbonate rocks: Geology, v. 19, p. 1093–1096.

Witts, J.D., Whittle, R.J., Wignall, P.B., Crame, J.A., Francis, J.E., Newton, R.J., and Bowman, V.C., 2016, Macrofossil evidence for a rapid and severe Cretaceous–Paleogene mass extinction in Antarctica: Nature Communications, v. 7, article 11738, doi: 10.1038/ncomms11738.

Zinsmeister, W.J., 1998, Discovery of fish mortality horizon at the K-T boundary on Seymour Island: re-evaluation of events at the end of the Cretaceous: Journal of Paleontology, v. 72, p. 556–571.

Zinsmeister, W.J., Feldmann, R.M., Woodburne, M.O., and Elliot, D.H., 1989, Latest Cretaceous/earliest Tertiary transition on Seymour Island, Antarctica: Journal of Paleontology, v. 63, p. 731–738.

Received 21 May 2020; accepted 22 December 2020.

FIGURES

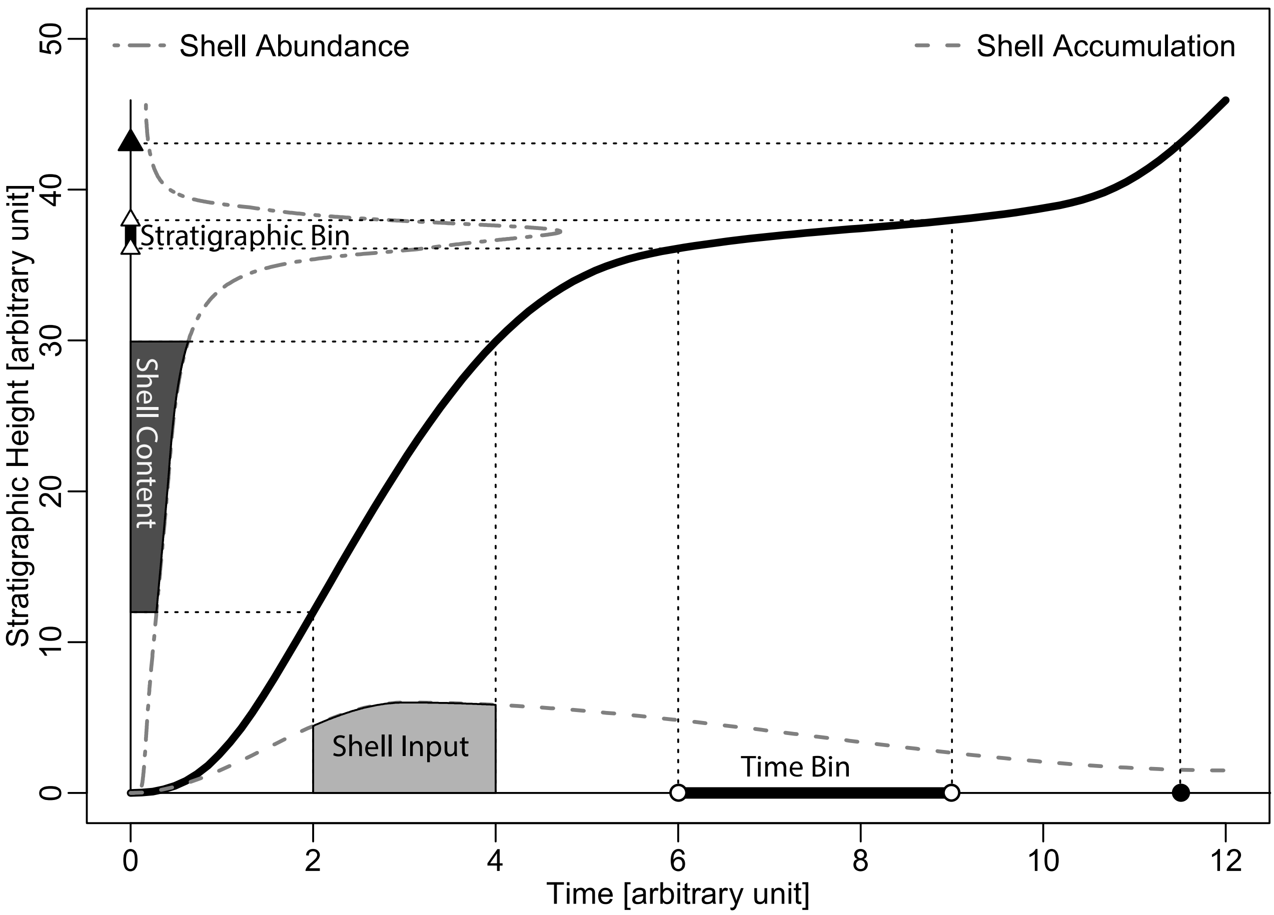

Fig. 1.—The transformations between time and stratigraphic height underlying the DAIME model. The age model or sediment accumulation history (thick black line) connects stratigraphic heights with their time of deposition. A specimen deposited in the sediment at time 11.5 (filled circle) will thus be located at a stratigraphic height of 43 (filled triangle). When the location of a specimen is constrained by a stratigraphic bin, its time of deposition

is constrained by the corresponding time bin obtained by transforming the endpoints of the stratigraphic bin (empty triangles) into time (empty circles). Accordingly any shell input in the sediment during a time bin (light gray area) is proportional to the shell content in the corresponding stratigraphic bin (dark gray area). This can be used to transform shell accumulation rates in time (dashed line) into shell abundance per stratigraphic height (dash-dotted line) and vice versa.

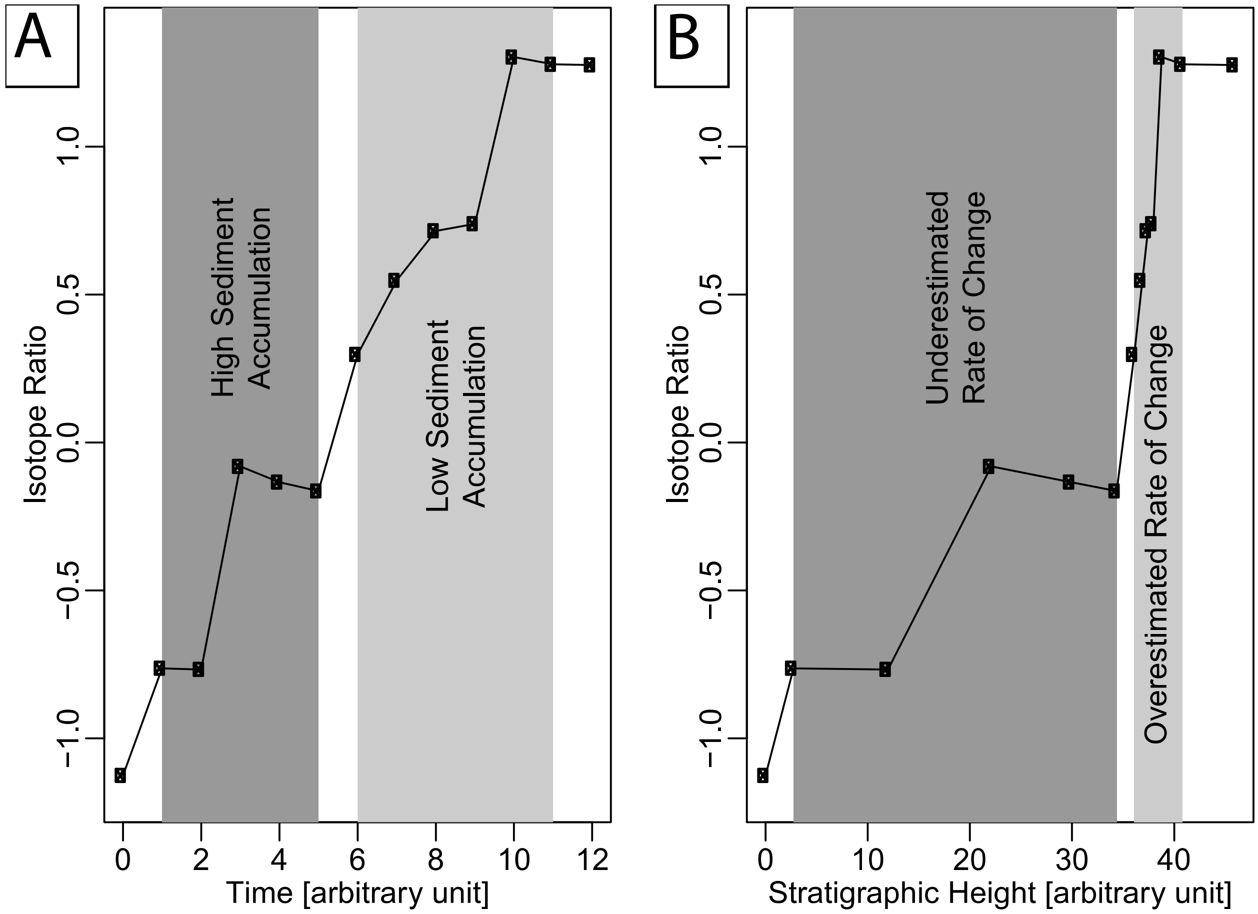

FIG. 2.—Samples associated with isotope ratios transformed based on the deposition model from Figure 1. **A**) In time. **B**) In stratigraphic height. Although the isotope ratios themselves are not altered, the distance between the samples changes due to sedimentary condensation or dilution when their stratigraphic heights are transformed into time. This leads to a “squeezebox effect”, where plots of isotope ratios, percentages, ratios, or any information that is associated with stratigraphic heights or times are a stretched or squeezed version of the original after the transformation, leading to an overestimate or underestimate of their rates of change.

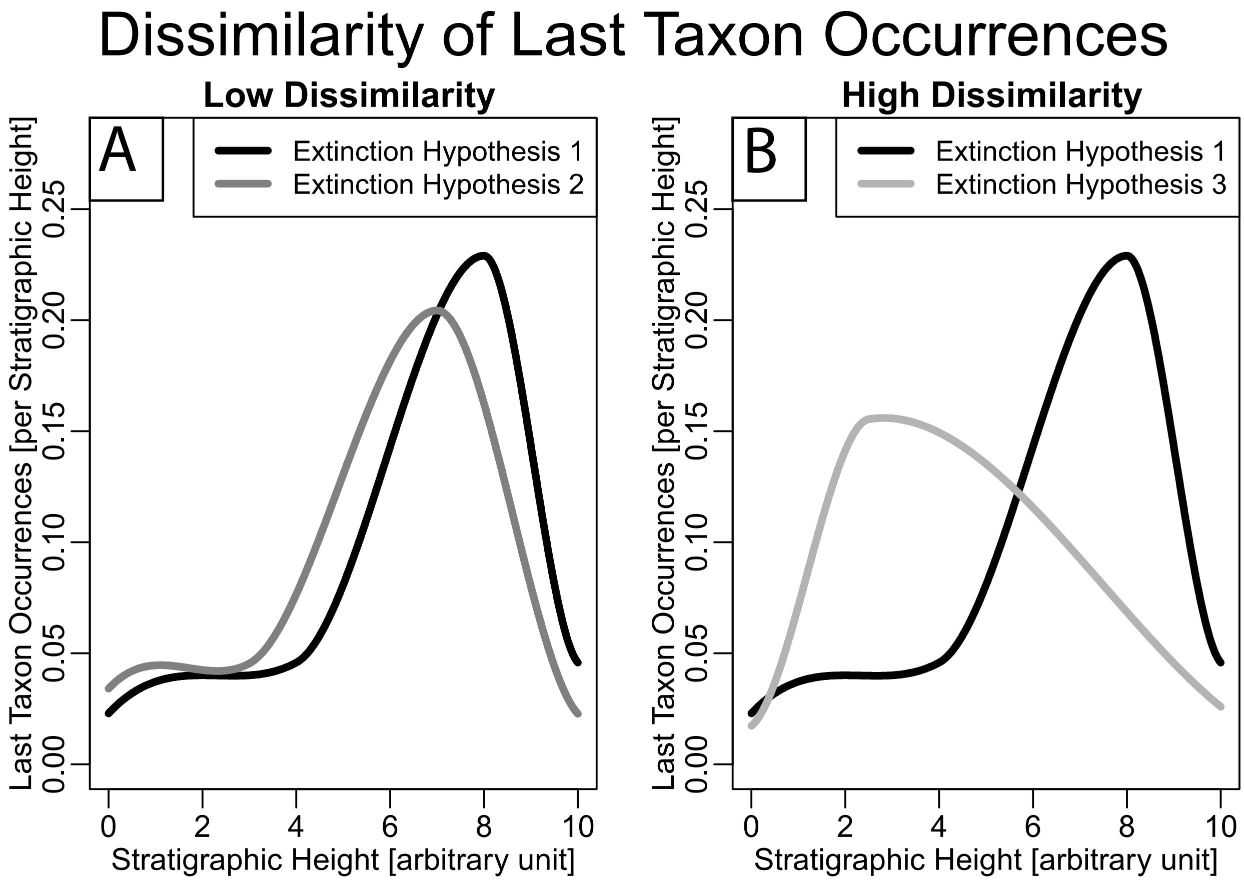

FIG. 3.—Stratigraphic patterns of last taxon occurrences (LTOs). **A**) High similarity. **B**) Low similarity. Each pattern corresponds to a different underlying extinction hypothesis. The symmetrized relative entropy is 0.34 for the dissimilar LTOs and 0.06 for the similar LTOs. Using pattern one as null hypotheses, the type 2 error half-life is 1.65 for the dissimilar LTOs, and 11.3 for the similar LTOs. Due to the exponential decrease of the type 2 error, this implies that at a sample size where type 2 error between the similar LTOs has halved, it has already decreased by a factor of more than 64 between the dissimilar LTOs.

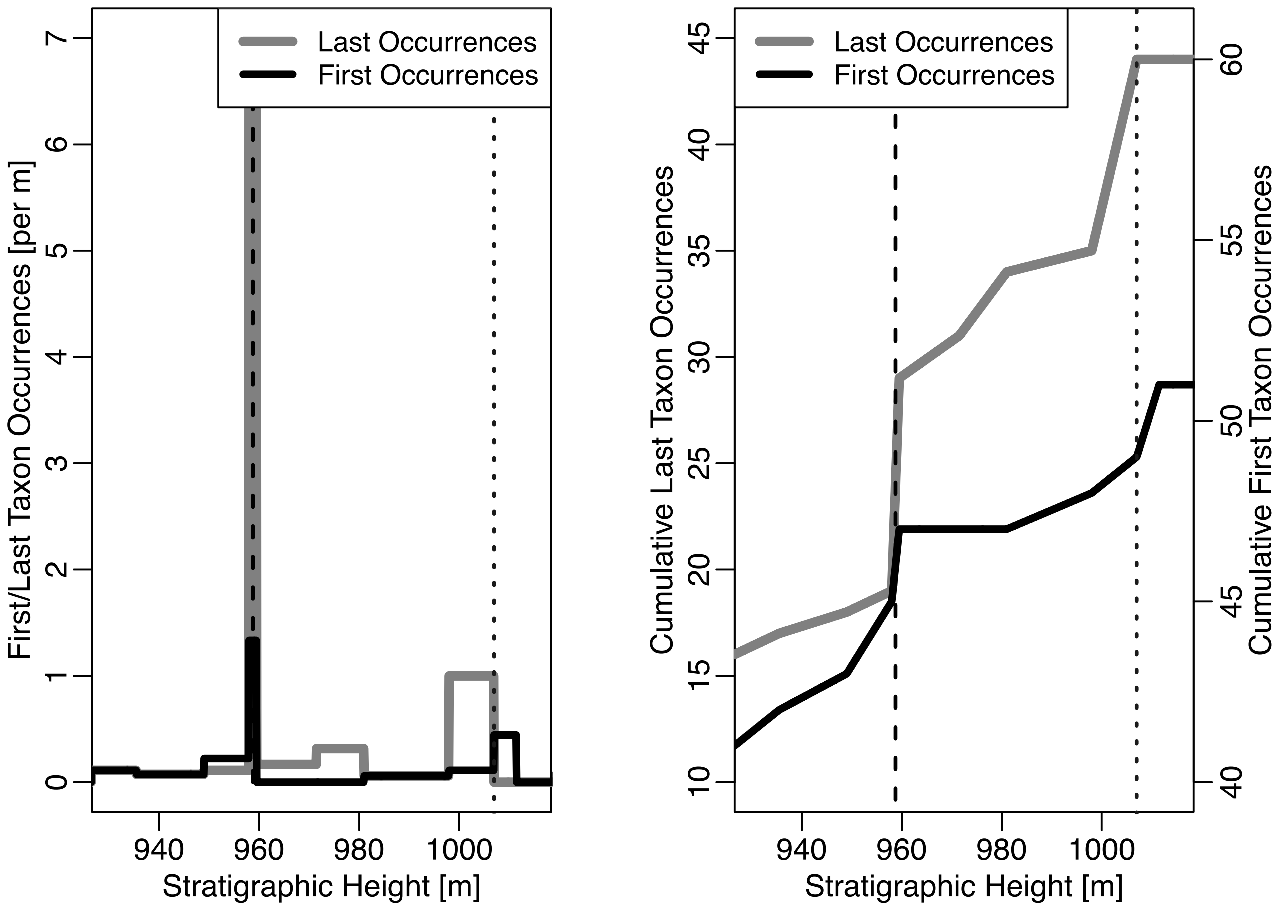

FIG. 4.—First and last taxon occurrences from Witts et al. (2016), section A. **A**) First and last taxon occurrences per meter. **B**) Cumulative first and last taxon occurrences in the section. Both modes of representation show an strong increase in last occurrences and a moderate increase in first occurrences around 959 m.

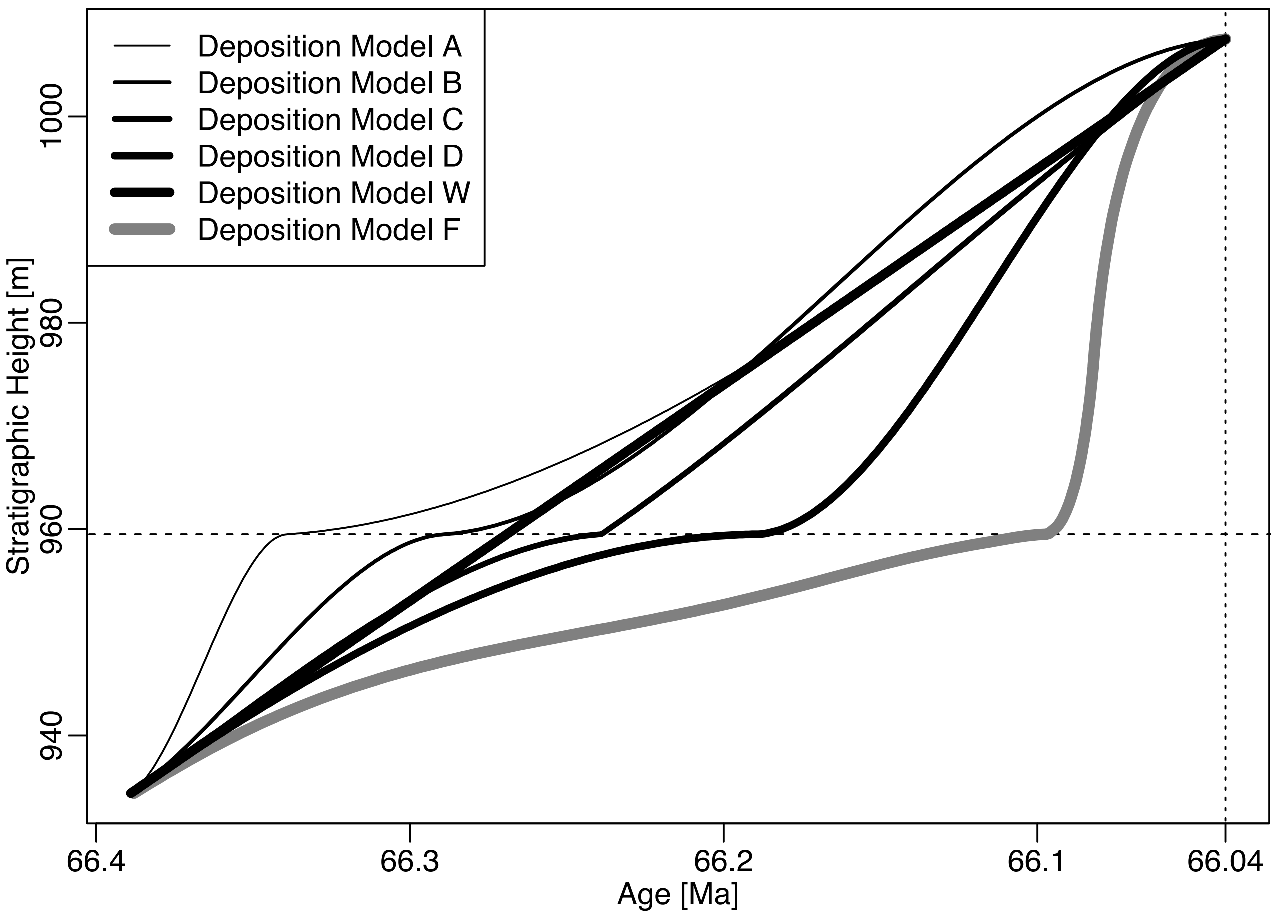

FIG. 5.—Five of the 33 deposition models for the K/Pg boundary as used in the example. The interval with low sediment accumulation rates is very short (A), short (B), intermediate (C), or long (D), the sediment accumulation rate at the K/Pg boundary is low (B) or average (A, C, D). During the interval with low sediment accumulation rates, sediment accumulation is very low (D) or low (A, B, C), after the interval it is either low (A, C, D) or average (B). Deposition model W is the "null model" of a constant sediment accumulation rate used by Witts et al. (2016). Deposition model F transforms the last taxon occurrences generated by an extinction hypothesis without any contribution of the early extinction interval into the stratigraphic pattern of an intermediate contribution of the early extinction pulse under deposition model D (see Fig. 7). The dashed line corresponds to the stratigraphic height of the peak in Figure 4, dotted line is the K/Pg boundary.

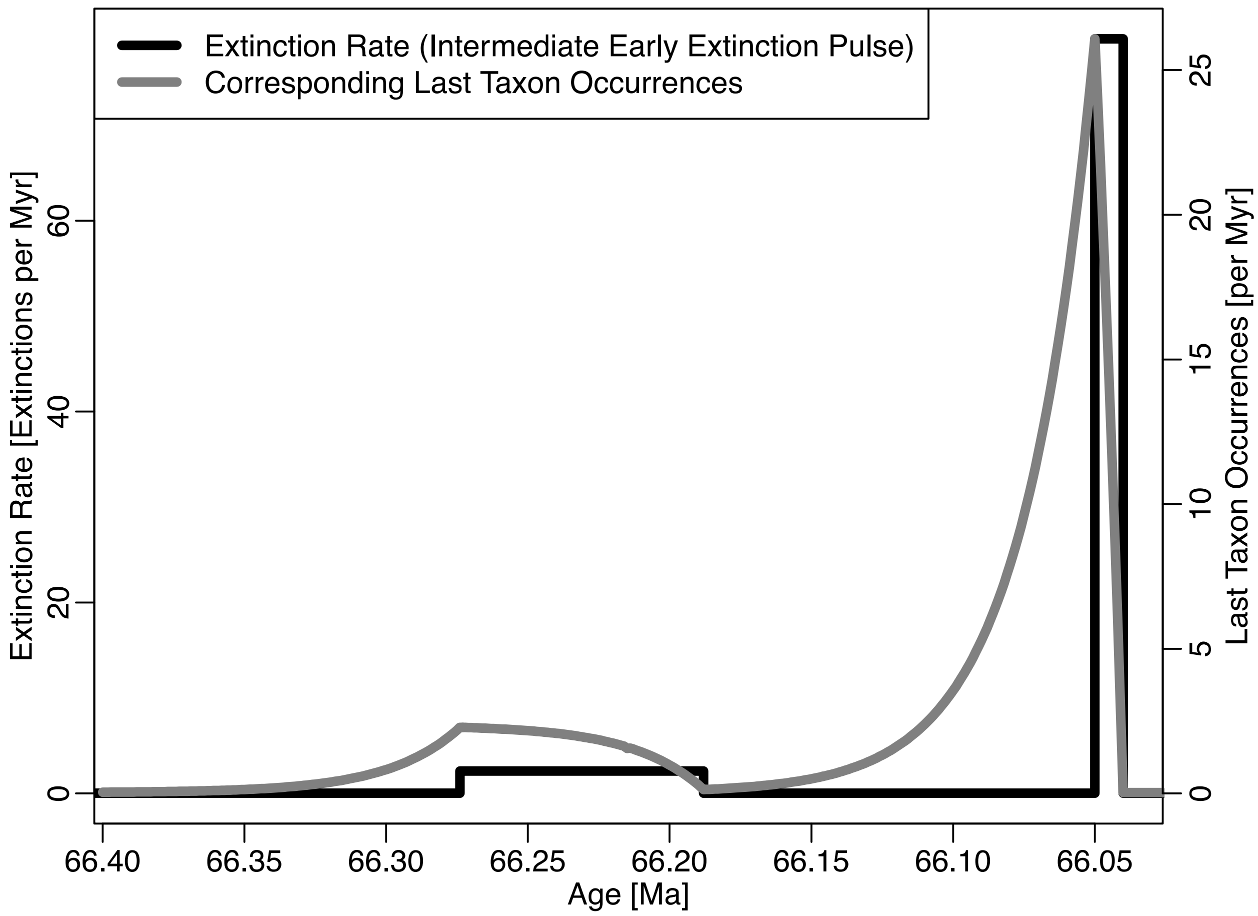

FIG. 6.—Extinction dynamic before and at the K/Pg boundary with early extinction pulse of intermediate intensity (black), and the last taxon occurrences in time generated by it (gray). Last taxon occurrences were derived based on the convolution procedure by Hohmann (2018) with a specimen frequency of 40 specimens per Myr, generating the characteristic "backwards smearing" of the Signor-Lipps effect. The timing of the early extinction pulse is based on the stratigraphic height of the extinction interval proposed in Tobin (2017), transformed into time by deposition model W from Figure 5.

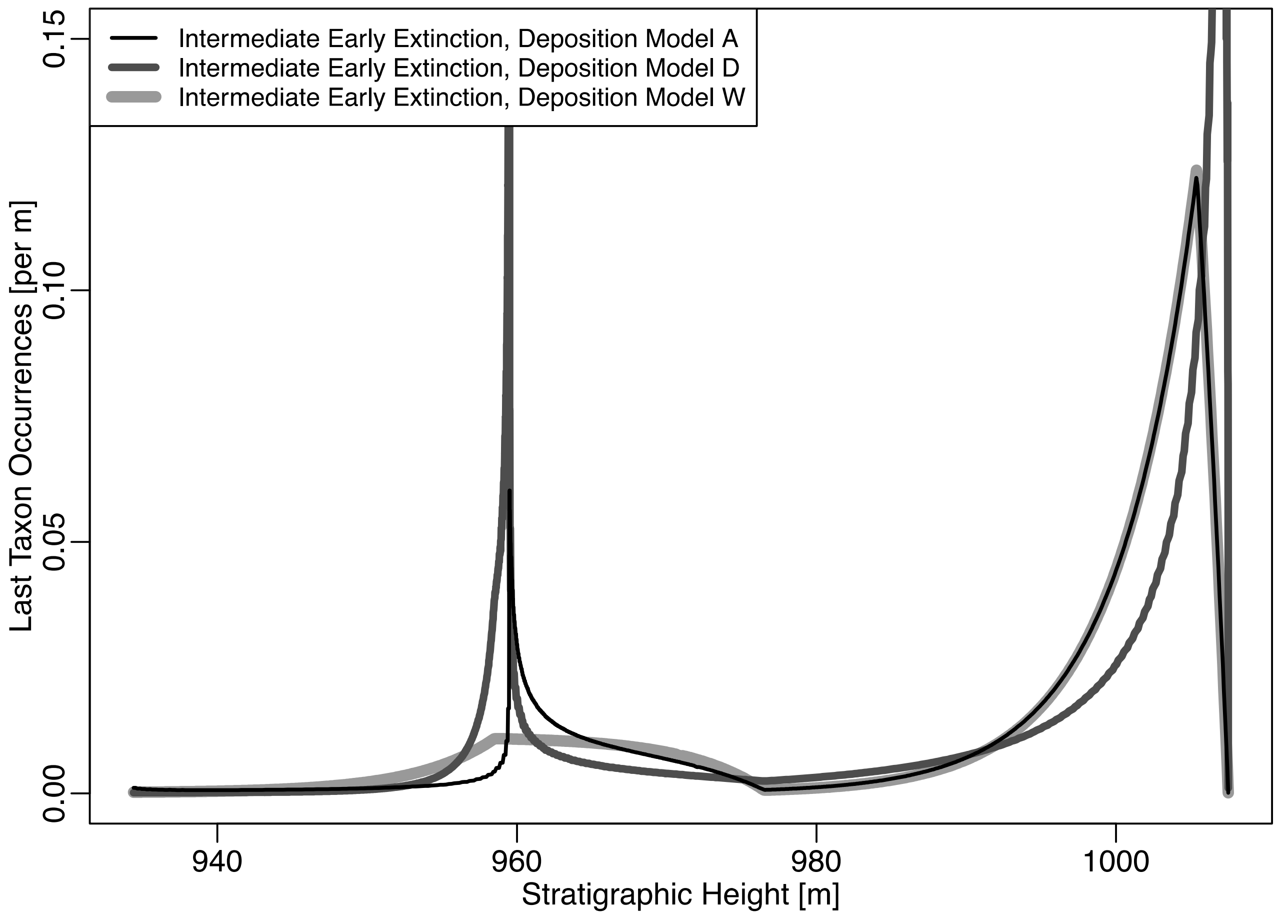

FIG. 7.—Stratigraphic expression of the extinction dynamics from Figure 6, based on the deposition models A (black), D (dark gray), and W (light gray) from Figure 5. The intensity of the early spike in last taxon occurrences reflects the duration of the low sedimentation interval (A = very short; D = long), a low sedimentation rate at the K/Pg boundary as in deposition model D generates sedimentary condensation that accentuates the extinction.

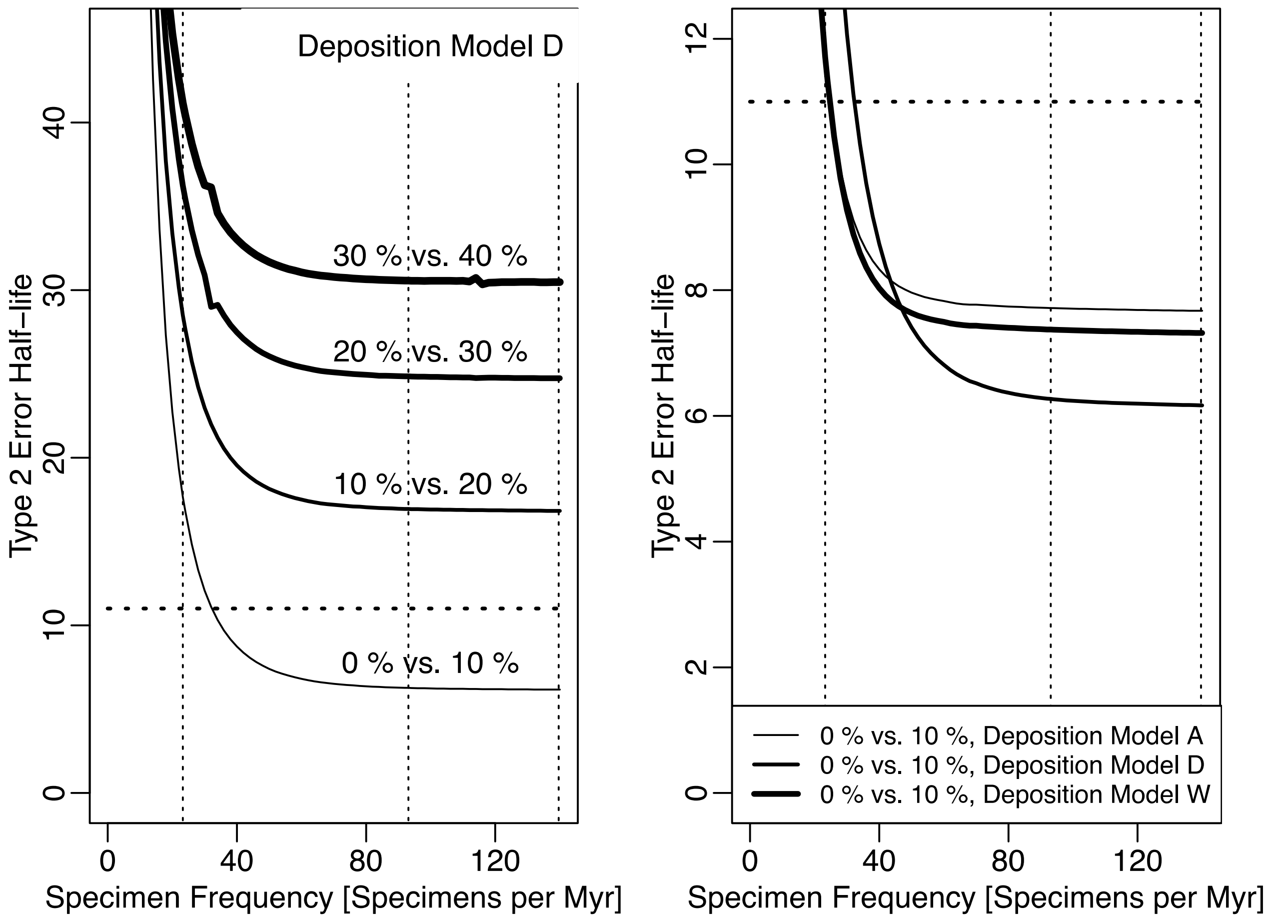

FIG. 8.—Difficulty to distinguish different intensities of the early extinction pulse. **A**) For different intensities under deposition model D. **B**) Between an absent and a weak early extinction pulse and for different deposition models. Recognizing a weak early pulse is easier than correctly assessing the intensity of a strong pulse (A), and the deposition model at hand has only a minor influence on this (given that knowledge about it is available, B). As reference for the specimen frequency, the vertical dotted lines show the specimen frequency of ammonite taxa from Witts et al. (2016) right before the K/Pg boundary in section A, transformed into time using the average sedimentation rate. As reference for the taxonomic richness of datasets used to infer about extinctions, the horizontal dotted line corresponds to the number of ammonite taxa in Macellari (1986).

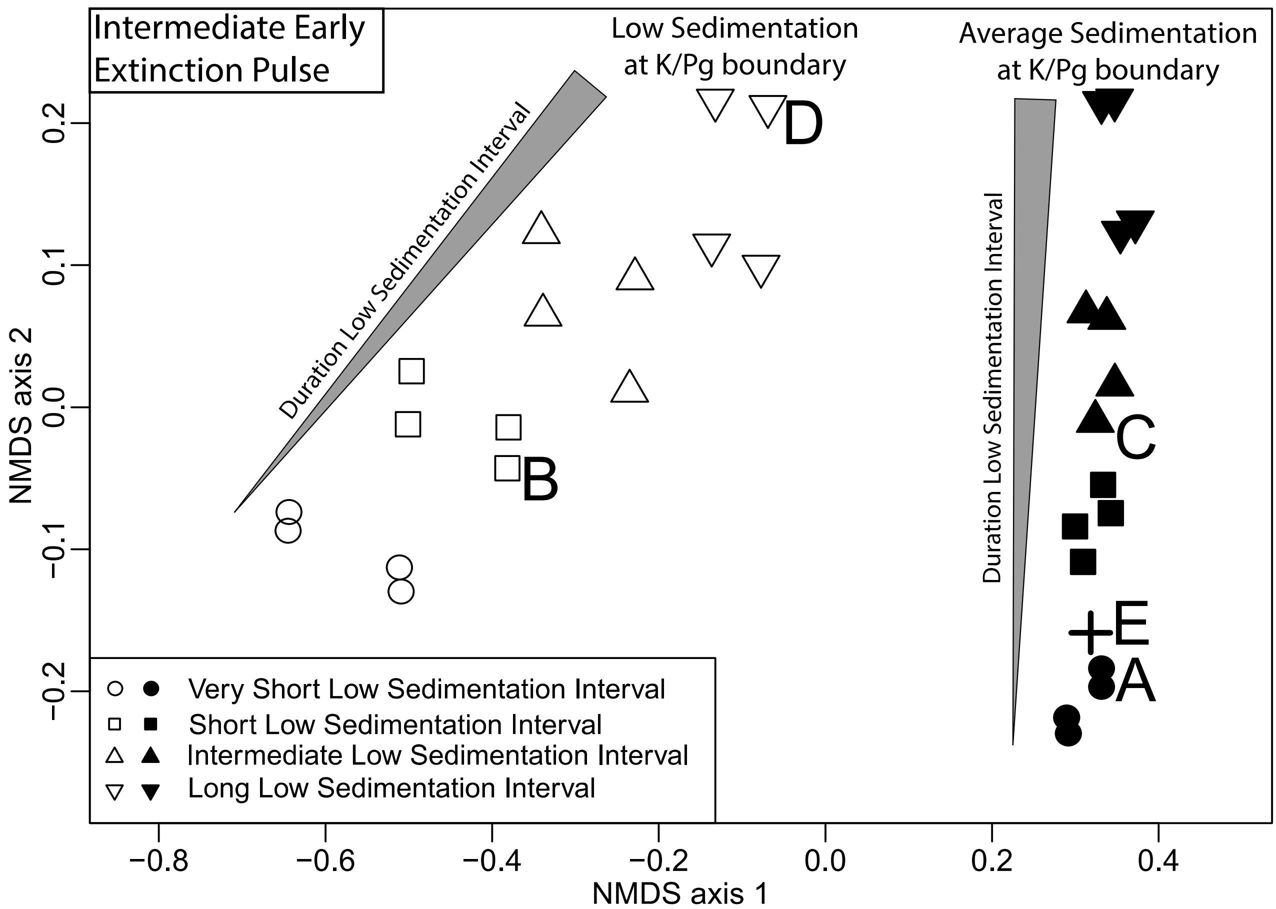

FIG. 9.—Dissimilarity of stratigraphic expressions of the K/Pg extinction with an intermediate early extinction pulse under different deposition models. Distance between age models in the NMDS corresponds to the dissimilarity of last taxon occurrences, generated by transforming extinction models with different age models. The letters correspond to the deposition models in Figure 5, specimen frequency is 40 specimens per Myr. Empty symbols have low sedimentation rates at the K/Pg boundary, filled average sedimentation rate. Key: circle = short interval; box = intermediate interval; triangle, tip up = long interval; triangle, tip down = very long interval with low sedimentation rate. The cross (W) corresponds to the deposition model with a constant sedimentation rate used by Witts et al. (2016). Stress of the NMDS is given in Appendix E.

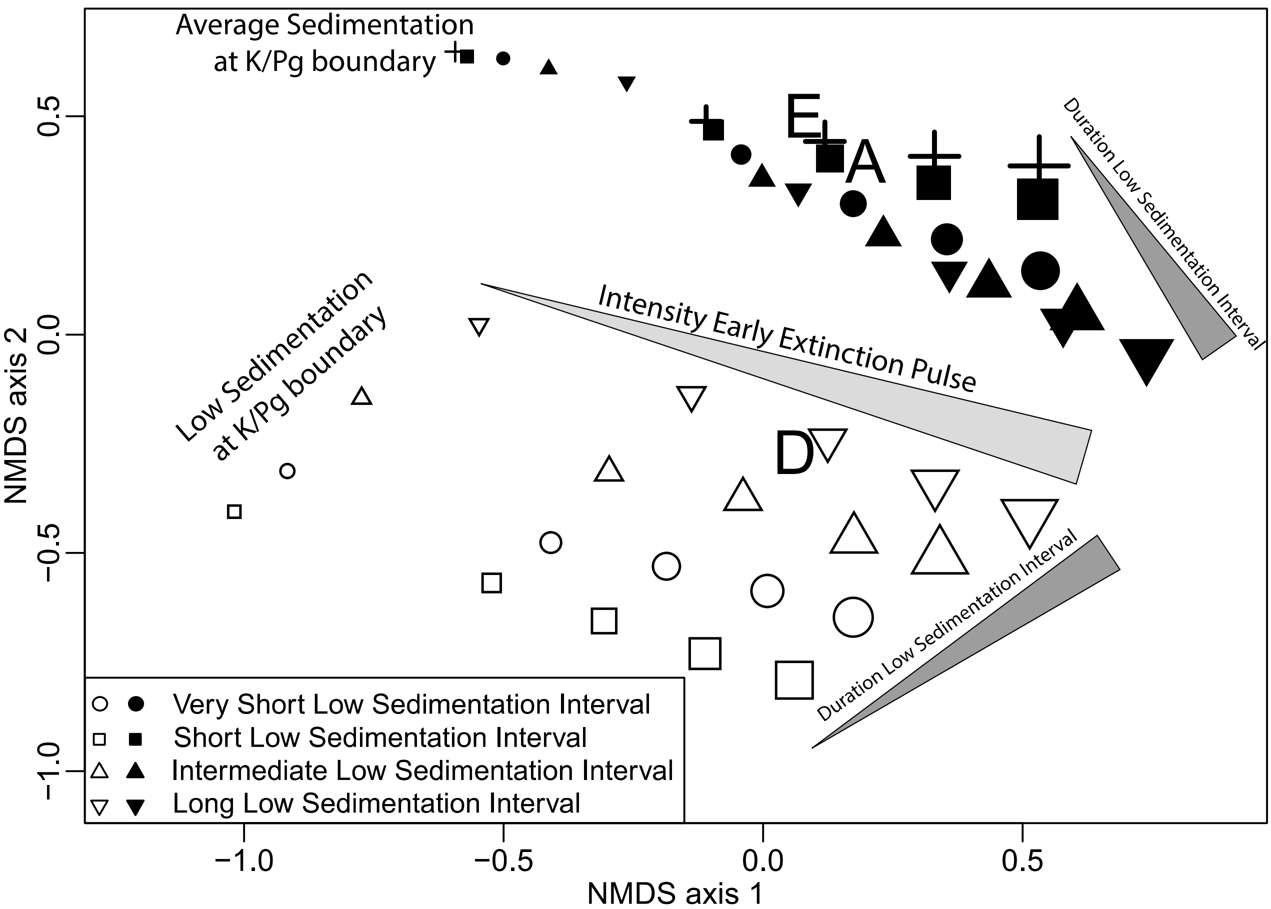

FIG. 10.—Dissimilarity of last taxon occurrences as a result of (1) the duration of the low sedimentation interval (2) sedimentation rate at the K/Pg boundary and (3) intensity of the early extinction pulse. Symbols are as in Figure 9, symbol size corresponds to the intensity of the early extinction pulse. Specimen frequency is 40 specimens per Myr, and all displayed age models have a very low sedimentation rate at the end of the low sedimentation interval as well as a low sedimentation rate after it. Stress of the NMDS is given in Appendix E.